Solar causes of the long-term increase in geomagnetic activity

JOURNAL OF GEOPHYSICAL RESEARCH, VOL. 104, NO. A12, PAGES 28,325–28,342, DECEMBER 1, 1999

Solar causes of the long-term increase in geomagnetic activity

R. Stamper, M. Lockwood and M. N. Wild

World Data Centre C-1 for Solar Terrestrial Physics, Rutherford Appleton Laboratory, Chilton, England, United Kingdom

T. D. G. Clark

British Geological Survey, Edinburgh, Scotland, United Kingdom

Abstract. We analyze the causes of the century-long increase in geomagnetic activity, quantified by annual means of the *aa* index, using observations of interplanetary space, galactic cosmic rays, the ionosphere, and the auroral electrojet, made during the last three solar cycles. The effects of changes in ionospheric conductivity, the Earth's dipole tilt, and magnetic moment are shown to be small; only changes in near-Earth interplanetary space make a significant contribution to the long-term increase in activity. We study the effects of the interplanetary medium by applying dimensional analysis to generate the optimum solar wind-magnetosphere energy coupling function, having an unprecedentedly high correlation coefficient of 0.97. Analysis of the terms of the coupling function shows that the largest contributions to the drift in activity over solar cycles 20-22 originate from rises in the average interplanetary magnetic field (IMF) strength, solar wind concentration, and speed; average IMF orientation has grown somewhat less propitious for causing geomagnetic activity. The combination of these factors explains almost all of the 39% rise in *aa* observed over the last three solar cycles. Whereas the IMF strength varies approximately in phase with sunspot numbers, neither its orientation nor the solar wind density shows any coherent solar cycle variation. The solar wind speed peaks strongly in the declining phase of even-numbered cycles and can be identified as the chief cause of the phase shift between the sunspot numbers and the *aa* index. The rise in the IMF magnitude, the largest single contributor to the drift in geomagnetic activity, is shown to be caused by a rise in the solar coronal magnetic field, consistent with a rise in the coronal source field, modeled from photospheric observations, and an observed decay in cosmic ray fluxes.

1. Introduction

The gradual growth in geomagnetic activity since the turn of the century, as quantified by the *aa* index, has been discussed by several authors [e.g., *Russell*, 1975; *Feynman and Crooker*, 1978; *Clilverd et al.*, 1998]. We know of this trend because of the work of *Mayaud* [1971, 1972], who retrospectively compiled the *aa* index from historic magnetometer data. Feynman and Crooker showed that for the years 1900-1968, the average *aa* values drifted by 0.22 nT yr^{-1} (giving a total drift over the period of the study of 15 nT), superimposed on a solar cycle variation of amplitude near 10 nT. This behavior can be seen in Figure 1, which extends the sequence up to the start of 1996. Figure 1a shows the variation of the yearly means of the daily *aa* values and Figure 1b shows the smoothed sunspot numbers, *R*. We do not here employ the extension to the sequence which has been derived using data from Helsinki [*Nevanlinna and Kataja*, 1993], nor the data from Sabine's Colonial Observatories [*Sabine*, 1857]. The period shown in Figure 1 begins just after the sunspot minimum prior to solar cycle 11 and ends at the sunspot minimum which marks the start of cycle 23 and thus covers almost 12 full solar cycles. In addition to the rise in geomagnetic activity since 1900, as seen in <*aa*>, the mean sunspot numbers (averaged over each solar cycle) have risen [*Russell*, 1975] and the solar cycles have also become shorter in length [*Friis-Christensen and Svensmark*, 1997].

There is a minimum of geomagnetic activity during solar cycle 14 (1902-1914), followed by a gradual rise. This rise is interrupted briefly by a decrease around the start cycle 20. This trend is also seen in the peak sunspot numbers. The sunspot number always returns to close to zero at each minimum, whereas the minimum <*aa*> has increased steadily since 1910 (with the one exception of the minimum at the start of cycle 20). Closer inspection of Figure 1 shows that there has been a gradual change in the phase difference between the variations in *R* and <*aa*>. For the minima at the start of cycles 12, 13, and 14 (1879, 1890, and 1902) the minima of <*aa*> and *R* are coincident. This was first noted by *Ellis* [1900], using data from the Greenwich magnetometer for solar cycles 9-13. However, after 1910 both the minima and maxima in <*aa*> are delayed compared with the corresponding troughs and peaks in *R* [*Fraser-Smith*, 1972]. This phase shift is largest for cycles 20 and 21 with a peak in <*aa*> for cycle 20 taking place only just before the subsequent minimum in *R* and the next minimum in <*aa*> being actually coincident with a peak in *R* for cycle 21. All cycles show peaks in <*aa*> during the declining phase [*Gonzales et al.*, 1990]. For <*aa*> this is the

Paper number 1999JA900311
0148-0227/99/1999JA900311$09.00

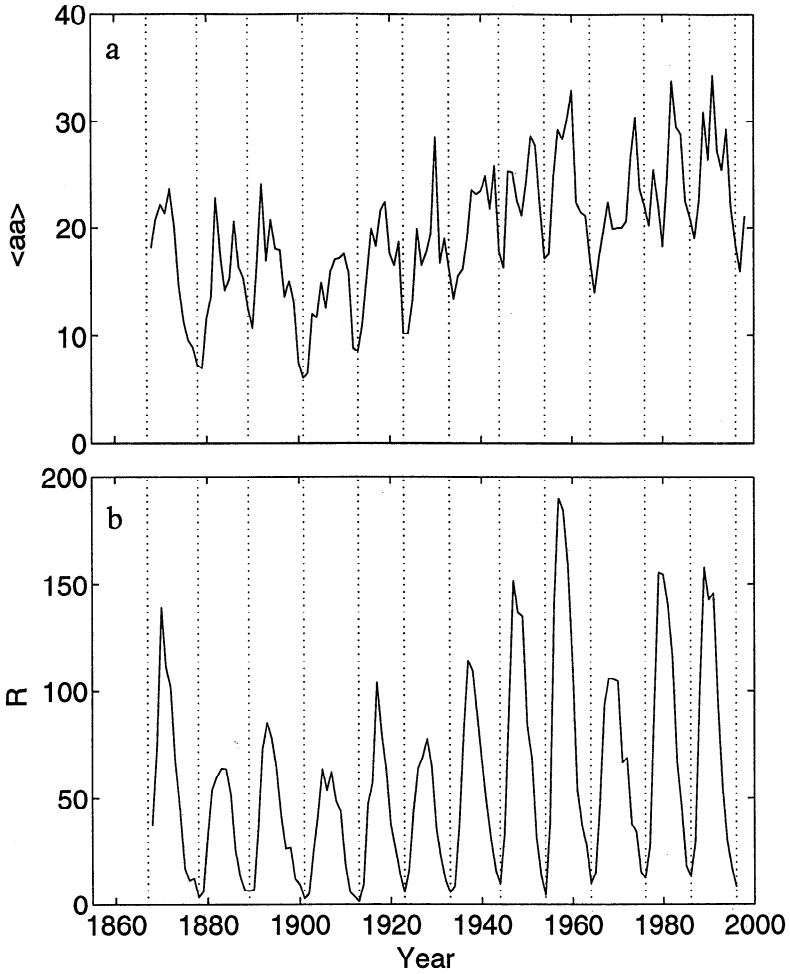

Figure 1. (a) Annual means of daily *aa* values, <*aa*> and (b) the smoothed sunspot number, *R* for 1868-1996. The dashed vertical lines show the years of sunspot minima.

dominant peak for all cycles except 12 and 13. A major component of these declining-phase peaks in geomagnetic activity are recurrent geomagnetic storms [e.g., *Clilverd et al.*, 1998] which are associated with long-lived fast solar wind streams [*Sheeley et a.l*, 1976; *Bame et al.*, 1976; *Mursala and Zieger*, 1996] and are strongest in the declining phase of even-numbered solar cycles [*Hapgood*, 1993; *Cliver et al.*, 1996]. The recurrent fast solar wind streams at Earth are associated with coronal hole extensions toward the solar equator [*Wang et al.*, 1996].

The similarities between the changes in *R* and <*aa*> are sufficient to suggest that the rise in magnetic activity on Earth arises from long time-scale variations of the sun, of which sunspots are one symptom. This correlation has been exploited by *Cliver et al.* [1998] who used *R* to estimate *aa* and the interplanetary conditions during the Maunder minimum of sunspot activity (circa 1645-1715). However, as pointed out by *Clilverd et al.* [1998], there are several other possible factors that must be evaluated, and a number of ways in which changes on the sun could have influenced the *aa* index data series. In this paper we analyse these factors in order to eliminate them.

1.1. Instrument effects

The *aa* index is defined as the average, for 3-hour intervals, of the *K* values of two near antipodal, midlatitude magnetometer stations. The *K* value depends on the range of the variation of the magnetic field strength in each 3-hour period after the quiet diurnal variation has been subtracted.

The exact location of the stations used has varied. Initially, Greenwich and Melbourne were employed. However, the Australian station was moved in 1919 to Toolangui and in 1980 to Canberra; the U.K. station was moved to Abinger in 1926 and to Hartland in 1957. For each change in location, a correlation analysis was carried out and calibration factors used to allow for changes in geomagnetic latitude and local induction effects. However, *Clilverd et al.* [1998] have pointed out that the drift of the geomagnetic poles has accelerated and that the distance of any one station from the average location of the auroral oval has changed as a result. However, the Australian stations have drifted poleward by ~2° since 1868, whereas the UK stations have drifted equatorward by ~4°. This might have added to the annual variation in *aa* but, if anything, would be expected to give a very minor decrease in the annual means <*aa*>. In addition, we note that the

sensitivity and accuracy of the magnetometers deployed have increased and the instruments have changed from analogue to digital.

1.2. Data Reduction Effects

Because much of the data was scaled by Mayaud (and the remainder done as a continuation of his work to more recent times), the background subtraction and range determination is thought to be effectively homogeneous for the entire data set. *Mayaud* [1971] showed that the diurnal variation was eliminated if 4 or more of the 3-hourly *aa* values are averaged together. We therefore first average the 3-hourly aa values into daily values; we then average out annual effects by averaging the daily values over a full year.

1.3. Ionospheric Effects

For a given electric field variation in time and space, the K value for either of the *aa* stations will depend on the ionospheric conductivities. Long-term drift in ionospheric conductivities could come about in a number of ways. The simplest would be caused by a drift in the E region plasma density, N_e. This can arise from changes in photoionizing solar EUV and X-ray fluxes, in particle precipitations, or in loss rates caused by thermospheric composition changes. However, the effects of conductivity variations are not clear. If, in relation to the currents detected by the *aa* magnetometers, the magnetosphere acts as a current source, this sets the magnitude of the Pedersen currents which close the field-aligned currents. The Hall currents would then depend on the ratio of the Hall and Pedersen conductivities, which is independent of N_e. Thus the E region plasma densities N_e would, in this case, influence the ionospheric electric fields but would not influence *aa*. On the other hand, if the magnetosphere acts as a voltage source, both the Hall and Pedersen currents would depend on the relevant conductivity. Thus, in this second case, *aa* would vary linearly with N_e. In addition, it is not clear where the currents detected by the *aa* magnetometers flow and thus to what extent the conductivity of the local ionosphere is relevant. The remote response to the large currents that can flow in the auroral oval means that there are often magnetic deflections (or "equivalent currents") at midlatitudes without there being significant local currents. Although conductivities in both the auroral oval and at midlatitudes are influenced by both particle precipitation and ionizing solar electromagnetic radiation, in the oval they are enhanced by particle precipitation to a much greater extent. Thus the local conductivity may be of limited relevance.

Changes in the ionospheric magnetic field B_i have more complex effects, as discussed by *Clilverd et al.* [1998], who concluded that the observed magnetic field changes will have reduced conductivities by only 3.7% since 1930 for the U.K. stations but increased them by ~2.2% for the Australian station. By comparison, over the same period, the rate of drift determined by *Feynman and Crooker* [1978] gives a change in <*aa*> of 15 nT which, given that the average value for cycle 16 (1923-1934) is 16.7 nT, is a change of 90%.

Long-term changes in the neutral thermosphere could also have changed the ionospheric conductivity profile by altering the collision frequencies. *Rishbeth* [1990] predicted that the peak height of the E layer would have fallen by ~2.5 km since 1900, in response to increased temperatures in the lower atmosphere, thought to be produced by anthropogenic effects, although also bearing a marked anticorrelation to the length of the solar cycle [*Friis-Christensen and Svensmark,* 1997]. These predictions of descending ionospheric layers have recently been verified by *Bremmer* [1998] and *Jarvis et al.* [1998]. Typical $N_e(h)$ altitude variations mean, however, that the effect on height-integrated conductivities is very small. Changes in the height of the conducting layer, whether introduced by changes in the ionospheric profile, the magnetic field, or the neutral thermosphere could, in principle, also alter the *aa* index via the range-squared term in the denominator of Biot-Savart's law. However, the above changes of order 2 km in magnitude would give only a 0.05% change in the magnetic deflection seen by even a local ground-based magnetometer.

1.4. Magnetospheric Effects

A long-term change in the ionospheric currents would call for changes in the magnetosphere because the field-aligned currents into and out of the ionosphere (responsible for transfer of the electric fields to the ionosphere and for the closure of the Pedersen currents) would be different. The general cause of field-aligned currents, and their intensification during magnetospheric substorm activity, is known to be the extraction of solar wind energy during periods of southward interplanetary magnetic field (IMF). It is possible that there has been a change in the magnetospheric response to a given level of energy input. The major response of the magnetosphere to this energy input is the substorm cycle, but the causes of substorm onset (namely the trigger for the diversion of cross-tail current into the ionosphere in the current wedge at the onset of the expansion phase) are not yet understood and are not predictable. One potential cause of a change in the magnetospheric response would be a change in the conditions needed for substorm onset. For example, some models of substorm onset invoke the presence of heavy ionospheric ions in the onset region, the fluxes of which are controlled by both the solar wind and solar electromagnetic radiations and could, in principle, have been subject to a long-term drifts caused by either influence.

Alternatively, the energy extracted from the solar wind may have changed. This could be caused by a change in the energy flux of the solar wind (dominated by the kinetic energy of the solar wind bulk flow), and/or a change in the efficiency with which the incident energy is extracted, and/or a change in the area that the magnetosphere presents to the solar wind flow. The fraction of the solar wind energy that is extracted is known to depend on the orientation of the IMF in a frame relative to the Earth's magnetic axis [*Hirshberg and Colburn,* 1969; *Russell and McPherron,* 1973; *Muryama and Hakamada,* 1975]. Hence the known drift in this axis [*Merrill et al.,* 1996] may be a factor. In addition, the observed long-term reduction in the Earth's magnetic moment should have reduced the area that the magnetosphere presents to the solar wind flow.

1.5. Interplanetary Effects

Long-term drifts in the IMF orientation, with respect to the ecliptic plane, and/or in the IMF magnitude will cause corre-

sponding changes to the solar wind-magnetosphere energy coupling function. Changes of the solar wind dynamic pressure, on the other hand, will cause two competing effects. The dynamic pressure corresponds to the kinetic energy density of the solar wind, but its increase would compress the magnetosphere and reduce the total area onto which that energy flux is incident.

Several past studies have looked at annual and semiannual means of parameters describing the solar wind and IMF at 1AU [e.g., *Gosling et al.*, 1976]. The solar cycle is the dominant influence on the variations of the interplanetary medium around the Earth [e.g., *Sheeley et al.*, 1976; *Webb and Howard*, 1994]. The best combination of the interplanetary parameters for quantifying the energy input into the magnetosphere (or at least of that part of the energy input that is relevant to geomagnetic activity) is not clear for timescales of half a year and greater. *Gringauz* [1981] found a strong correlation between annual means of *aa* and the solar wind speed v_{sw}, whereas *Snyder et al.* [1963] and *Crooker et al.* [1977] found that geomagnetic activity is closely related to its square, v_{sw}^2. These studies employed data from solar cycle 20 only. On short timescales, v_{sw} is almost constant and so the effect of the IMF orientation was found to exert a dominant influence [*Schatten and Wilcox*, 1967; *Arnoldy*, 1971] (plus see review by *Baker* [1986]). More recently, *Crooker and Gringauz* [1993] and *Schreiber* [1998] have shown that the correlation of annual or semiannual averages of geomagnetic activity with v_{sw}^2 begins to break down after 1976 and that the IMF orientation is a factor for the data during solar cycle 21, even for longer timescales. This change was attributed to the larger magnitude of IMF B_z variations in cycle 21 [*Slavin et al.*, 1986; *Hapgood et al.*, 1991]. For short (minute to hour) timescales, much work has been done to find the form of the coupling function that best predicts the Auroral Electrojet index, *AE*. Some of the concepts developed for these high timeresolution studies are applied to the yearly averages for three solar cycles in section 3 of this paper.

1.6. Solar Effects

Changes in the interplanetary medium in which the Earth's magnetosphere is immersed may mean that the Sun itself has changed or that the position of the Earth in the (otherwise constant) heliosphere may have altered. For example, a shift in the magnetic neutral line in the solar corona [*Bravo and Stewart*, 1994] would cause a change in the average IMF and solar wind at Earth [*Rosenberg and Coleman*, 1969]. Observations have revealed much about the three-dimensional structure of the heliosphere in recent years [*Luhmann et al.*, 1993; *Balogh et al.*, 1995; *Wang and Sheeley*, 1995; *Gazis*, 1996] and variations seen near Earth over the sun's full 22-year cycle have been explained in terms of the location relative to the heliospheric current sheet (the extension of the coronal neutral line). Although the inclination of the coronal neutral line shows a strong solar cycle variation, there is no evidence for a long-term drift [*Hoeksema*, 1992].

1.7. Evaluation of Possible Effects

In this paper, we analyze the series of *aa* index values in an attempt to see which of the potential long-term effects, discussed in sections 1.1-1.6 above, are causes of the long-term drift in geomagnetic activity seen in Figure 1. To do this, we also employ *E* region ionospheric data from the Slough ionosonde (starting 1931 and so covering solar cycles 17-22), the auroral electrojet index, *AE* (starting 1958), observations of cosmic ray fluxes (starting 1953) and data from near-Earth interplanetary space (starting 1964 and covering solar cycles 20, 21, and 22).

2. Analysis of Long Data Sequences From Ground-Based Observatories

We here normalize data to allow easy comparison of different data series and to understand the effects of the solar cycle. For any parameter X, we compute X^* given by

$$X^* = \{ X - \langle X \rangle \} / \sigma_X , \quad (1)$$

where $\langle X \rangle$ is the mean of X and σ_X is the standard deviation for the total period studied. We apply equation (1) to X values that are annual means of daily averages. Figure 2a shows the values of aa^* for 1868 to 1996 (solid line). Also shown is the variation of the normalised sunspot number R^* (dashed line). Figure 2b shows the variation of the difference between these two normalized data sequences ($aa^* - R^*$) and reveals that the overall drift in geomagnetic activity, as quantified by *aa*, is very similar to that in the sunspot number, R (because ($aa^* - R^*$) stays close to zero on average). The trend for the $\langle aa \rangle$ oscillations to grow out of phase with R and increasingly to lag behind R, can be seen by the increasing amplitude of the quasi 11-year cycle in ($aa^* - R^*$). The peaks in ($aa^* - R^*$) occur in the declining phase of the solar cycles, when $\langle aa \rangle$ tends to remain high compared to the sunspot numbers. The minima in ($aa^* - R^*$) arise from the rising phases when $\langle aa \rangle$ remains relatively low. This phase shift reached a maximum in cycles 20 and 21, when $\langle aa \rangle$ peaks only shortly before the minimum in R and then is a minimum at the next solar maximum.

Close inspection reveals that ($aa^* - R^*$) is generally negative before 1900 but is positive for much of the recent solar cycles, indicating that the fractional upward drift in $\langle aa \rangle$ is somewhat larger than that in R. This is shown more clearly in Figure 3 which plots running means of the normalised values, R_{11}^* (dashed line) and aa_{11}^* (solid line). The averages are computed for 11-year periods around each year, such that the solar cycle variations are smoothed out. It can be seen that the rise in mean aa_{11}^* is similar to, but slightly larger than, that in the normalized sunspot number R_{11}^*. In both cases, there are clear rises in the intervals 1900-1955 and 1965-1996, with a marked decrease between 1955 and 1965.

2.1. Comparison With Ionospheric Observations

The longest continuous sequence of ionospheric data is for the Slough/Chilton sites, close to the northern hemisphere magnetometers used to construct the *aa* index (and also used to produce the a_n index). As for the magnetometer data, cross-calibration of data from the Chilton and Slough sites was made from 2 years of joint operation prior to the move to Chilton. Given that the correlation of the data from the two sites was very high, the data from these two stations form an effectively continuous sequence stretching back to 1930. We generate daily means of the hourly measurements of the *E* region critical frequency *foE*. These daily means of *foE* are converted into peak plasma densities N_mE and then are treated in the same way as the daily *aa* values; that is, they are used to give the annual means. The changes in the average *E* region

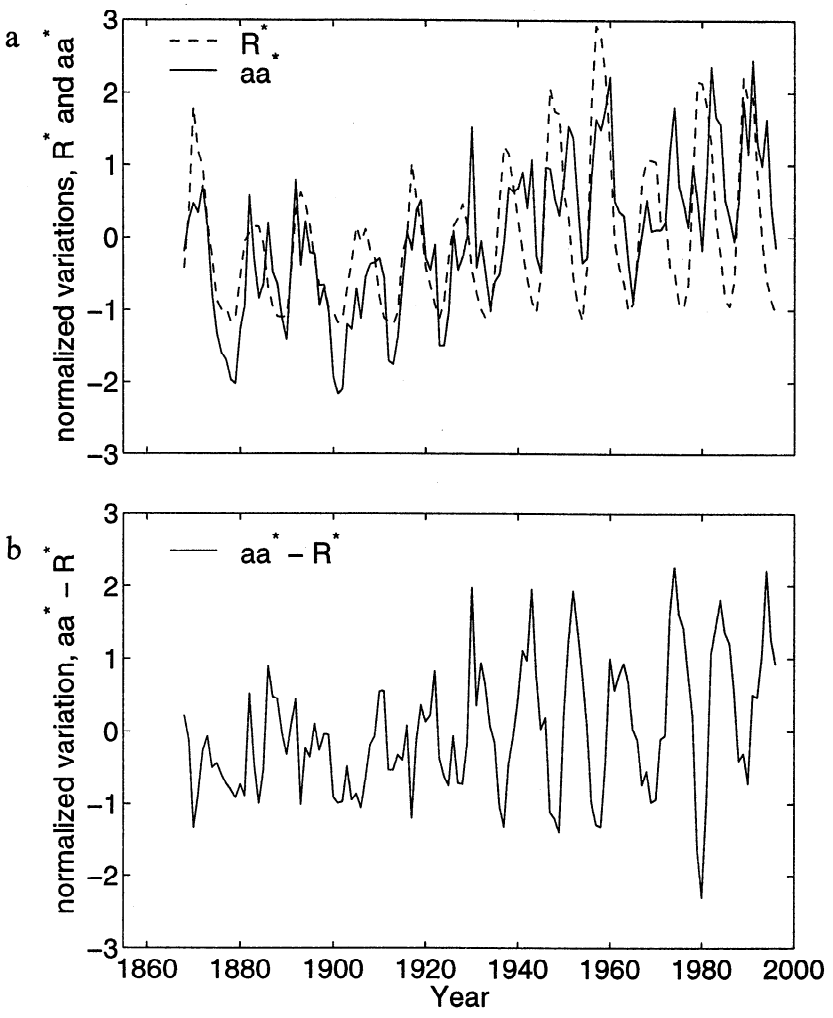

Figure 2. (a) The normalized *aa* index *aa** (see equation (1) of text) for the years 1868-1996 (solid line) and the normalized sunspot number *R** (dashed line). (b). The difference (*aa**-*R**).

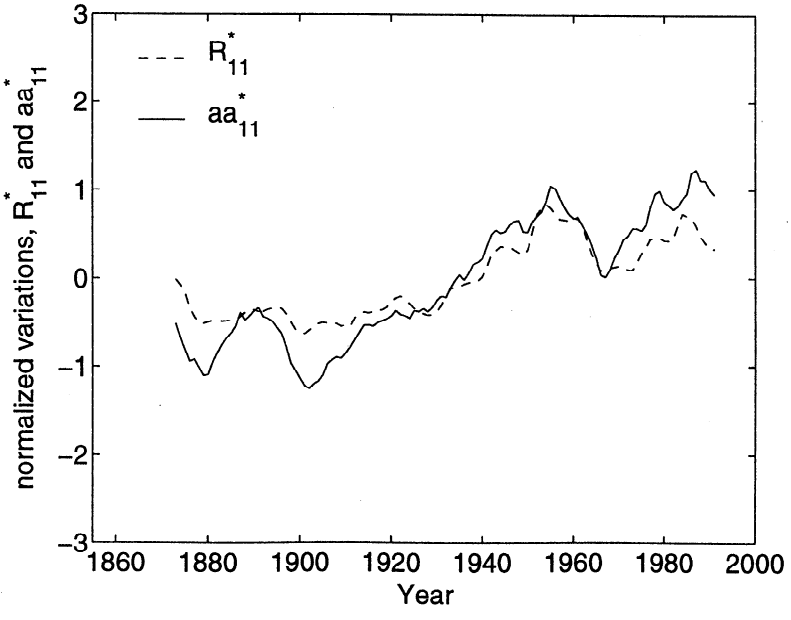

Figure 3. The 11-year running means of the normalized values annual means for the *aa* index, aa_{11}* (solid line) and sunspot number, R_{11}* (dashed line).

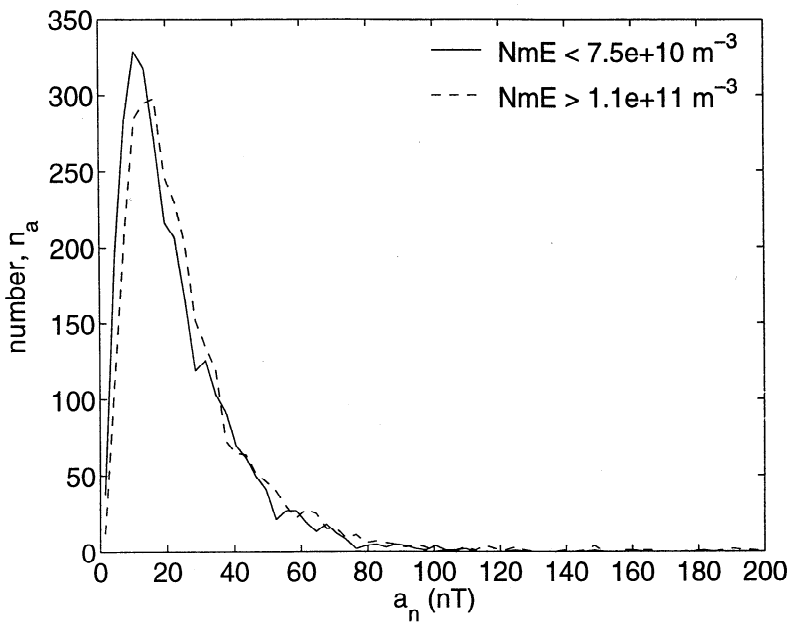

Figure 4. The distributions of daily means of a_n , $n(a_n)$ for two ranges of N_mE in the local ionosphere: are $N_mE < 7.5\times10^{10}$ m^{-3} and $N_mE > 1.1\times10^{11}$ m^{-3} (i.e., less than lower quartile and greater than the upper quartile, respectively), shown as solid and dashed lines.

peak densities since 1930 are generally consistent with the increase in the average sunspot number R, given by the regression equation [*Allen*, 1948]:

$$N_mE = (3.3/8.98)^2 \{(1+0.008R)\cos\chi\}^{1/2}, \quad (2)$$

where χ is the solar zenith angle, which becomes a function of only the station latitude and time of year when the daily averages are taken and of latitude only when annual means are taken.

To investigate the influence of these ionospheric changes on the *aa* index, we here use the a_n index, compiled from the K values from the same northern hemisphere magnetometers as used to generate *aa*. We restrict the data to 1964 onward, to be consistent with the study presented in the next section. Figure 4 shows two distributions of observed a_n values for two ranges of daily averaged N_mE, as observed by the nearby Slough/Chilton ionosonde. These ranges are $N_mE < 7.5\times10^{10}$ m^{-3} (solid line) and $N_mE > 1.1\times10^{11}$ m^{-3} (dashed line) which are, respectively, the lower and upper quartiles of the N_mE distribution. For each of the two N_mE ranges, the number of times the daily mean of a_n falls in bins 3 nT wide, $n(a_n)$, is plotted. It can be seen that the distribution $n(a_n)$ is not influ-

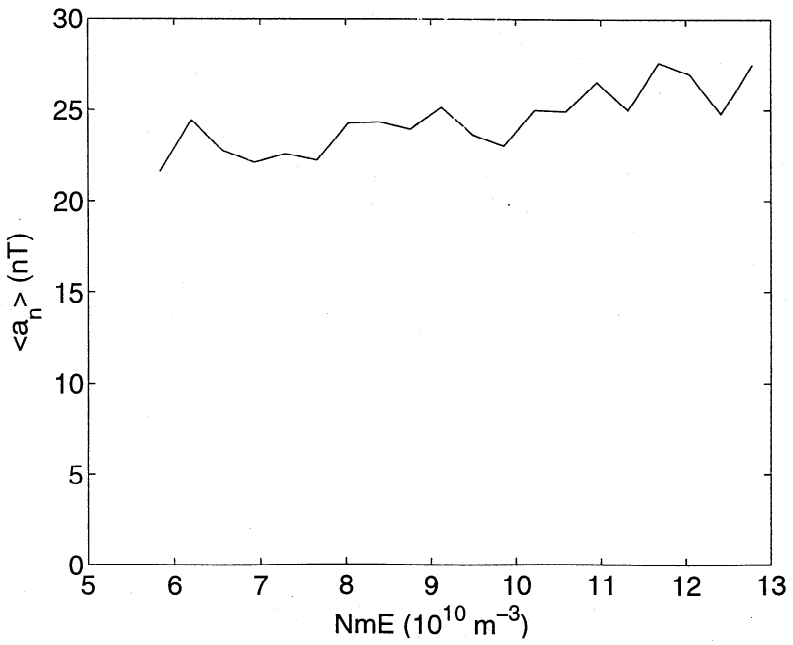

Figure 5. The mean values of a_n averaged over 20 bins of daily mean N_mE between the two five percentile points of the N_mE distribution. A regression fit gives a slope of $s_{an} = 6.560 \times 10^{-11}$ nT m^{-3} .

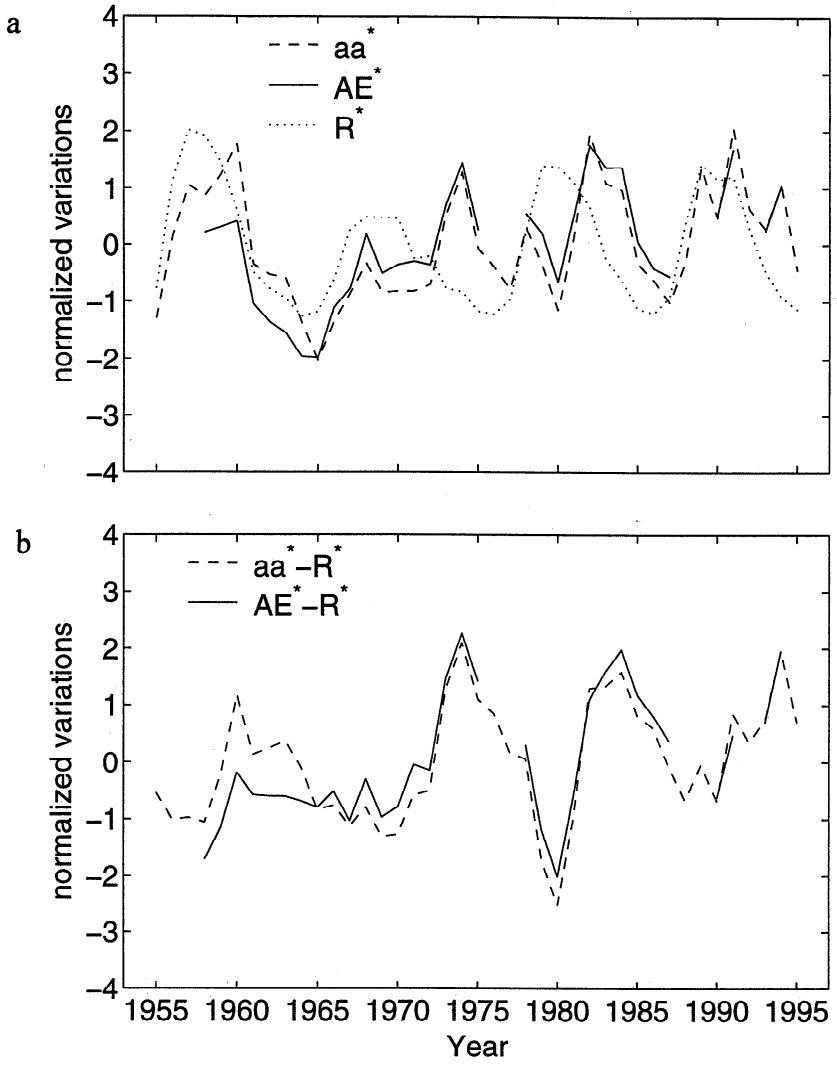

Figure 6. (a) The normalized annual means of the *aa* index, *aa** (dashed line), of the *AE* index, *AE** (solid line), and of the sunspot number, *R**, (dotted line) for the period 1955-1996. (b) the differences {*aa*-R**} (dashed line) and {*AE*-R**} (solid line). Note there are some gaps in the AE data sequence.

enced by the local N_mE for a_n greater than 36 nT. Thus the local E region densities do not influence the occurrence of the more active periods (for example the storms with $aa > 40$ nT studied by *Clilverd et al.* [1998]). This either implies that the magnetosphere is effectively a current source in these disturbed cases and/or that the *aa* magnetometers are responding to currents in the auroral oval where conductivities are no longer well correlated with those at Slough. By equation (2), the part of the conductivities caused by photoionization (as opposed to particle precipitation) should correlate well at different sites, and this is probably the reason why the local E region densities are clearly a factor in the distribution of the lower a_n values. The mode value of a_n rises from 10 to 16 nT with the increase in N_mE. At these lower a_n therefore the magnetosphere is acting more like a voltage source. Because of the effect at low magnetic activity, the mean of a_n (averaged over all activity levels) will depend on the local E region density. To see this effect, Figure 5 plots the average values of a_n for 20 bins of daily averaged N_mE between the two five-percentile points. A clear but slight upward trend can be seen. A regression fit to Figure 5 gives a slope of $s_{an} = \{\partial\langle a_n\rangle/\partial N_mE\} = 6.560 \times 10^{-11}$ nT m^3.

2.2. Comparison With *AE* Index Observations

Since 1958, the Auroral Electrojet (*AE*) index has been compiled from a ring of 12 stations around the northern hemisphere auroral oval [*Davis and Sigura*, 1966; *Baumjohann*, 1986]. In addition to the *AE* magnetometers being much closer to the main site of energy deposition, *AE* is not an index based on *K* values and so is unlike *aa* and *Ap*. Figure 6a shows the normalized annual means of the *aa* index, *aa** (dashed line), of the *AE* index, *AE** (solid line), and of the sunspot number, *R**, (dotted line) for the period 1955-1996. (Note that the *R** and *aa** values need to be recalculated for each interval studied as the mean and standard deviation will depend on the interval selected.) Figure 6b shows the differences (*aa*-R**) and (*AE*-R**), as dashed and solid lines, respectively. It is immediately apparent that on these annual timescales, the *aa* index is an excellent representation of *AE*, particularly for the period 1964-1996 studied in the next section. This is significant because we can eliminate the possibility that the *aa* index is not a reliable indicator of energy deposition in the auroral ovals on these long timescales. Specifically, changes associated with the locations of the stations

and the way the index is compiled can be ruled out. We also note that annual means of *aa* and the planetary *Ap* index are also highly correlated [*Crooker and Gringauz*, 1993].

3. Analysis of Data From Interplanetary Space

Since 1963, we have a reasonably continuous sequence of in situ data on the interplanetary medium around the Earth. These data now cover three full solar cycles (numbers 20, 21, and 22). This is a short period compared to the 100 years over which the level of magnetic activity has gradually increased. However, the interplanetary data do cover cycles 20 and 21, for which the phase shift is greatest (Figure 2). In addition, the interplanetary data cover a period in which there is a consistent drift to higher values in <*aa*> (Figures 1 and 3). Analysis of the three solar cycles of joint interplanetary and *aa* index data should allow us to identify if, and to what extent, the changes are due to changes in the interplanetary medium around the Earth. In making such a study one must bear in mind that the nature of the interplanetary medium is such that several parameters are strongly intercorrelated [*Bowe et al.*, 1990; *Scurry and Russell*, 1991]. We also note that the rise in *aa* seen in cycles 20, 21, and 22 is not a simple continuation of the drift seen during cycles 14-19, there being a clear decrease around the start of cycle 20 (1955-1965). However, thereafter, the rise in <*aa*> has all the characteristics of the rise seen earlier in the century.

We employ annual means of interplanetary data from 1964 to 1995, inclusive. The minumum of the smoothed sunspot number between cycles 19 and 20 was in August 1964, whereas that between cycles 22 and 23 was in August 1996. Thus we are using data which commence 7 months before a sunspot minimum and end 7 months before another minimum, and so these data cover three full solar cycles.

Many studies have used high time resolution data on the interplanetary medium and correlated with geomagnetic data of similar resolution. In particular, *AE* index values of resolution between 1 min and 1 hour have been used. A variety of coupling functions which aim to describe the energy transfer from the solar wind to the magnetosphere have been proposed and tested (see review by *Baker* [1986]). We here adopt the dimensional analysis introduced by *Vasyluinas et al.* [1982], because it gives us a physics-based means of studying the origins of long-term changes. They noted that the power extracted from the solar wind, P_α, is the product of three terms:

$$P_\alpha = (\pi l_o^2)(m_{sw} N_{sw} v_{sw}^3/2)(t_r) \quad (3)$$

The first term in brackets on the right-hand side is the area (a circle of radius l_o) that the magnetosphere presents to the solar wind flow. The second term in brackets is the flux density of kinetic energy in the solar wind flow, where m_{sw} is the mean ion mass, N_{sw} is the solar wind density and v_{sw} is the solar wind speed. The third term is "transfer function", t_r, which is the fraction of the power incident on the magnetosphere that is extracted. A hemispherical shape for the dayside magnetopause is assumed, for which l_o is the stand-off distance of the nose of the magnetosphere and can be computed from pressure balance of the geomagnetic field with the solar wind dynamic pressure P_{sw} (= $m_{sw} N_{sw} v_{sw}^2$) [*Schield*, 1969].This yields a value for l_o proportional to $(M_E^2/ P_{sw} \mu_o)^{1/6}$, where M_E is the magnetic moment of the Earth. We adopt the dimensionless form of the transfer function suggested by Vasyluinas et al., with the $\sin^4(\theta/2)$ dependence on the IMF clock angle θ (in the GSM frame of reference) verified, for example, by *Scurry and Russell* [1991]:

$$t_r = k_1 (1/M_A^2)^\alpha \sin^4(\theta/2), \quad (4)$$

where k_1 is a dimensionless constant, M_A is the solar wind Alfvén Mach number (equal to $\{\mu_o P_{sw}\}^{1/2}/B_{sw}$, where B_{sw} is the strength of the interplanetary magnetic field) and α is called the coupling exponent. Substituting for each term in (4) and (5) yields

$$P_\alpha = \{k\pi /2\mu_o^{(1/3+\alpha)}\} m_{sw}^{(2/3-\alpha)} M_E^{2/3} N_{sw}^{(2/3-\alpha)} v_{sw}^{(7/3-2\alpha)} B_{sw}^{2\alpha} \sin^4(\theta/2). \quad (5)$$

To find the coupling exponent, α, geomagnetic activity is assumed to be proportional to the power extracted from the solar wind P_α. There are two factors to note about this assumption. First, the dependence of <*aa*> on the magnetospheric power input from the solar wind need not necessarily be one of proportionality and it may not even be linear. Second, whether proportional or not, there may have been a long-term drift in ionospheric conductivity and/or in the magnetospheric response.

It should be noted that a different definition of α has been employed by *Kan and Akasofu* [1982] and *Muryama* [1982] and we will call this α'. Comparison of the full definitions of the coupling functions reveals $\alpha = (1-\alpha')$. *Kan and Akasofu* [1982] show that if we neglect the variation of l_o with P_{sw} and employ $\alpha = 1$ ($\alpha'=0$), then P_α becomes the epsilon factor proposed by *Perreault and Akasofu* [1978] and *Akasofu* [1981] ($\varepsilon = k\, v_{sw} B_{sw}^2 \sin^4[\theta/2]$). However, ε was originally based on the interplanetary Poynting flux incident on the magnetopause, which does not allow for the fact that currents in the bow shock and magnetosheath make these regions sources of Poynting flux. From analysis of interplanetary and geomagnetic data, *Kan and Akasofu* [1982] derived a value of $\alpha = 1$ ($\alpha' = 0$) but did not allow for the variation in the area of the magnetospheric cross section. On the other hand, regression analysis allowing for this factor by *Bargatze et al.* [1986] found α near 0.5, while *Muryama* [1982] found $\alpha = 0.4$ ($\alpha' = 0.6$).

We here apply this functional form to the annual means. In computing P_α using equation (5), we employ the hourly averages of IMF and solar wind data (in GSE coordinates) from the "Omnitape" set supplied by NASA's NSSDC [*Couzens and King*, 1986]. These data were gathered by more than 10 satellites (e.g., IMP 8, ISEE 3, VELA) and at a variety of locations. The data set has been carefully compiled to cross-calibrate the data from different detectors. Although some questions remain about the absolute calibration of the observations prior to 1974 of, for example, N_{sw} and P_{sw} [*Gazis*, 1996], there is no doubt that this is the most homogeneous data set available. We assume that the composition of the solar wind, and thus the mean ion mass m_{sw}, is constant. To compare with <*aa*> values spanning the years 1964-1996, we here allow for the drift in the Earth's magnetic moment, M_E [*Merrill et al.*, 1996] in computing values of P_α. In addition, we compute the IMF clock angle θ, in the GSM frame of reference, for each hourly average of the IMF observations, using the prevailing orientation of the magnetic axis of the Earth derived from the IGRF model. Use of the correct dipole axis orientation could be important for these long-term studies be-

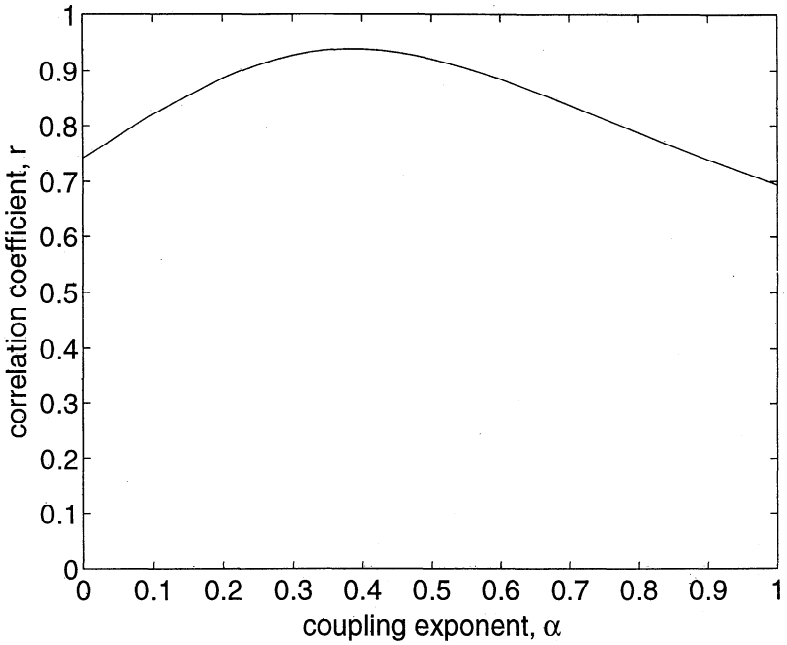

Figure 7. The correlation coefficient r between the 32 annual means of $<aa>$ and the annual means in P_α (computed from interplanetary data using equation (5)) for the period 1964-1996, shown as a function of the coupling exponent, α. The peak r is 0.94, which arises at a value of α of 0.386. Correlations of r exceeding 0.61 are significant at over the 99.99% level, those of r exceeding 0.525 are significant at the 99.90% level.

cause the magnetic poles are now moving faster than at any time since geomagnetic monitoring began. We here derive a value of each interplanetary parameter for each hour which, like the *aa* values, are averaged into daily values and then to annual means. Both the magnetic moment and the orientation of the GSM frame were computed using the IGRF model, using the coefficients relevant to the time of observation.

Figure 7 shows the correlation coefficient r between the 32 annual means of $<aa>$ and the annual means of P_α as a function of α. The peak r is 0.938, which arises at a value of $\alpha = \alpha_m = 0.386$. Considering that we are dealing with annual means, this value for the optimum α is surprisingly similar to those found for the higher time resolution studies, which were in the range 0.4-0.5.

All correlations shown in Figure 7 are significant at over the 99.99% level. Table 1 compares this correlation coefficient, and its significance, with others for other solar wind/IMF coupling functions. The third column, labeled chance, is the probability (as a percentage) that the correlation was obtained by chance (the significance level would be 100% minus this number). The coupling functions used are B_s, the southward IMF ($B_s = -B_z$ if $B_z < 0$, $B_s = 0$ if $B_z > 0$), v_{sw}^2, P_{sw}, $v_{sw} B_s$, $v_{sw}^2 B_s$, ε, and P_α for $\alpha = \alpha_m$ (giving the peak r), P_m. Note that B_s can also be expressed as $B_s = -U(\theta) B_{sw} \cos\theta$ where $U(\theta)$ is a half-wave rectification function ($U(\theta)=1$ if $\theta \geq \pi/2$, but $U(\theta)=0$ if $\theta < \pi/2$). In Table 1 each average is computed in two ways, labeled a and b in column 1. For method a, the annual mean of each parameter is computed and the means combined

Table 1. Correlations of Annual Means of Interplanetary Coupling Functions With $<aa>$

	Interplanetary coupling function	Correlation coefficient, r	chance (%)
a, b	$<B_s>$	0.519	0.12
a	$<v_{sw}>^2$	0.656	2.3×10^{-3}
b	$<v_{sw}^2>$	0.663	1.8×10^{-3}
a	$P_{sw} = <N_{sw}><v_{sw}>^2$	0.698	4.4×10^{-4}
b	$<P_{sw}> = <N_{sw} v_{sw}^2>$	0.743	5.5×10^{-5}
a	$<v_{sw}><B_s>$	0.747	4.5×10^{-5}
b	$<v_{sw} B_s>$	0.741	6.2×10^{-5}
a	$<v_{sw}>^2 <B_s>$	0.855	2.3×10^{-8}
b	$<v_{sw}^2 B_s>$	0.869	5.6×10^{-9}
a	$\varepsilon = <v_{sw}><B_{sw}>^2 <\sin^4(\theta/2)>$	0.827	2.8×10^{-7}
b	$<\varepsilon> = <v_{sw} B_{sw}^2 \sin^4(\theta/2)>$	0.781	6.9×10^{-6}
a	$P_m = <M_E>^{2/3} <N_{sw}>^{(2/3-\alpha m)} <v_{sw}>^{(7/3-2\alpha m)} <B_{sw}>^{2\alpha m} <\sin^4(\theta/2)>$	0.938	1.3×10^{-13}
b	$<P_m> = < M_E^{2/3} N_{sw}^{(2/3-\alpha m)} v_{sw}^{(7/3-2\alpha m)} B_{sw}^{2\alpha m} \sin^4(\theta/2) >$	0.938	1.3×10^{-13}
a	P_m (1974-1996, coincident data only)	0.967	4.1×10^{-12}

to give the coupling function. For method b, the hourly interplanetary parameters are combined to give a coupling function value for each hour and these are then averaged to give the annual means. The averaging is done in the same way as for <*aa*>. Very similar r and α_m were found by the two averaging procedures for P_m.

The magnitude of the peak correlation for P_m of $r = 0.94$ is similar to, but significantly larger than, those found by a number of other studies of annual and semiannual means (see review by *Feynman* [1983]). An even larger correlation coefficient of 0.95 was obtained for P_m if, in computing <*aa*>, we employ only *aa* values for times (roughly 50% of the full interval) when interplanetary data are available. This implies that the correlation is somewhat limited by the availability of IMF data. A further small increase can be obtained if we required linearity, but not proportionality, of <*aa*> and P_α (i.e., we allowed a nonzero intercept value of <*aa*> when $P_\alpha = 0$). As mentioned above, there are some questions concerning the calibration of the solar wind data prior to 1974. If we exclude these data, the peak correlation coefficient rises to an unprecedentedly high value of $r = 0.97$ (for $\alpha_m = 0.31$, which is somewhat lower than for the full period). This correlation means that 93% of the variation of the annual means of *aa* can be explained by the variations in the interplanetary medium.

Crooker et al. [1977] found that the *Ap* geomagnetic index increased as v_{sw}^2 and obtained a correlation coefficient of 0.86. However, these studies only employed data from before 1976. More recently, *Crooker and Gringauz* [1993] have shown that the correlation of yearly averages of geomagnetic activity with v_{sw}^2 begins to break down after 1976 and that the IMF orientation is a factor for the data from solar cycle 21. This change was attributed to the larger magnitude of IMF B_z variations in cycle 21 [*Slavin et al.*, 1986; *Hapgood et al.*, 1991]. *Crooker and Gringauz* [1993] obtained a correlation coefficient of 0.90 with (v_{sw}^2 B_s) with *Ap*, the variation of which is almost identical to that in *aa* on these timescales. This correlation was obtained using data from all of cycles 20 and 21, but only the start of cycle 22. Table 1 is for a longer period that covers all of cycles 20, 21, and 22, and we find that the correlation coefficient for v_{sw}^2 has fallen further still to 0.66 and that for (v_{sw}^2 B_s) has fallen to 0.85 (for method a) or 0.87 (for method b).

It is interesting to note that extending the data sequence to cover an extra solar cycle has not only improved the quality of the best correlation (from 0.86 to 0.90 to 0.97), but it has changed the form of the best fit coupling function. Equation (5) with $\alpha = \alpha_m = 0.386$ means that P_m varies as $v_{sw}^{1.56}$ instead of the v_{sw}^2 employed by *Crooker and Gringauz* [1993], and that their IMF term B_s ($= -U(\theta)B_{sw}\cos\theta$) is replaced by $B_{sw}^{0.77}$ $\sin^4(\theta/2)$. In addition, a dependence on $N_{sw}^{0.28}$ has been introduced.

From a regression fit of <*aa*> against P_m, we can evaluate the constant k, and so can use equation (5) to synthesize a predicted annual *aa*, aa_p, given by

$$aa_p = (1.8432 \times 10^{-17}) \langle M_E \rangle^{2/3} \langle N_{sw} \rangle^{0.28} \langle v_{sw} \rangle^{1.56} \langle B_{sw} \rangle^{0.77} \langle \sin^4(\theta/2) \rangle, \text{ nT} \quad (6)$$

where M_E is in Tm^3, N_{sw} is in m^{-3}, v_{sw} is in km s^{-1}, and B_{sw} is in nT.

Figure 8 shows the regression fit of <*aa*> with predicted value using equation (6), aa_p, and Figure 9 shows the variations of <*aa*> (solid line) and aa_p (dashed line). It can be seen that aa_p, and thus the best fit input power, P_m, matches the observed <*aa*> sequence extremely well and reproduces both its drift to larger values and its phase shift with respect to the sunspot number R. The main deviations are a few data points in cycle 20, early in the sequence. These may relate to the less certain calibration of these data points or may be due to the unusual nature of cycle 20, as discussed by *Gosling et al.* [1977], *Crooker and Gringauz* [1993], and *Hapgood et al.* [1991].

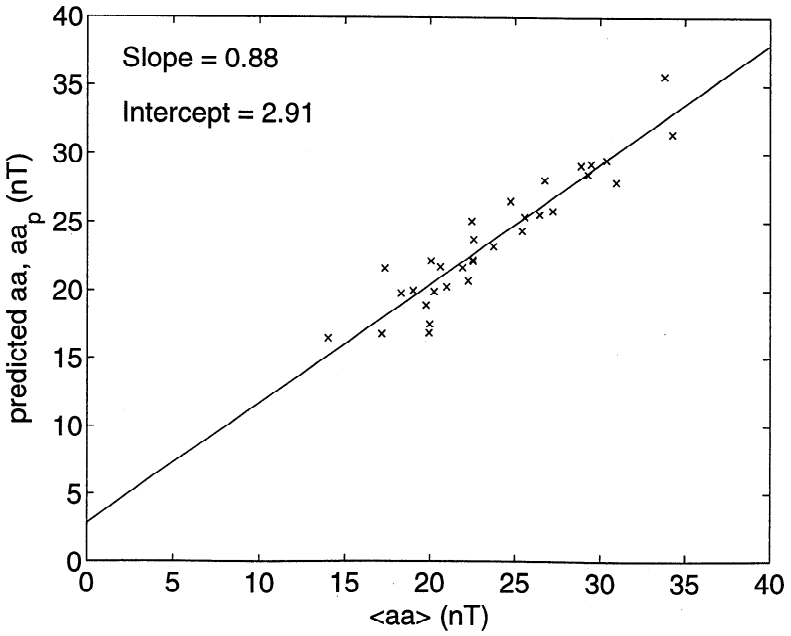

Figure 8. Regression fit of <*aa*> against predicted *aa*, aa_p (given by equation (6)), which is proportional to the best fit coupling function P_m (given by equation (5)).

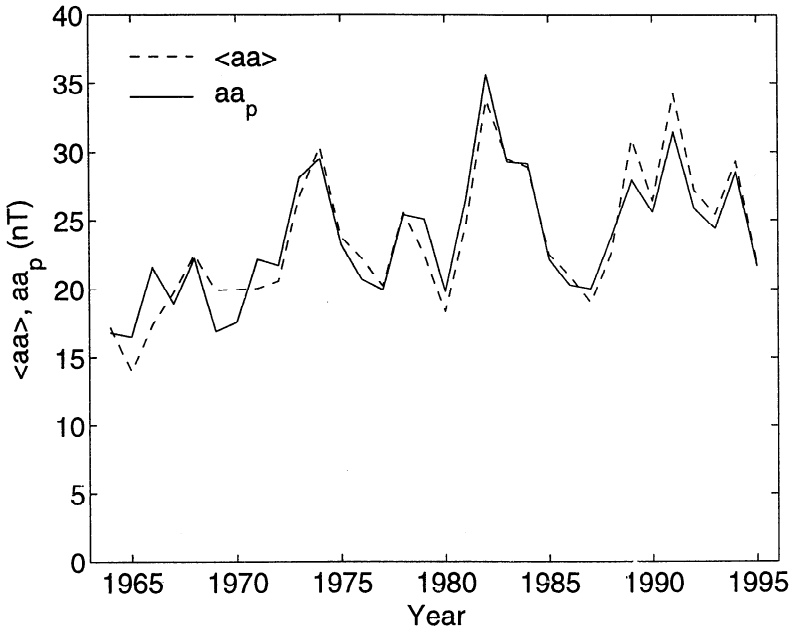

Figure 9. The variations of mean and predicted *aa*, <*aa*>, and aa_p (dashed and solid lines, respectively).

That we have reproduced the phase shift and drift in the <*aa*> values with P_m, enables us to evaluate the behavior of each of the terms that make up P_m. This is done in the next section. Note that by using the form given in equation (5), we have maintained proportionality of <*aa*> with each of the terms on the right-hand side. A slightly higher correlation was possible with a linear, but not proportional, expression and this would have been more difficult to analyze in terms of the origin of the long-term drift.

4. Evaluation of the Components in the Best Fit Coupling Function

We wish to determine the cause of the long-term drift in <*aa*> and the origin of the phase shift relative to the sunspot number. Figure 10 shows the variations of all the terms on the right-hand side of equation (5) for the best fit α. Because we have no indication of a long-term drift in the composition of the solar wind, we here assume that the mean ion mass, m_{sw}, is constant. The helium abundance in the solar wind varies between ~3% and 5% over solar cycle 20 [*Neugebauer*, 1981]. This corresponds to a mean ion mass variation between ~1.09 and 1.15 amu and the term $m_{sw}^{(2/3-\alpha_m)}$ in equation (4) therefore introduces a percentage variation of only ±0.75 % into P_m for the bestfit α found in the previous section.

Figure 10 shows the variations of $\langle M_E \rangle^{2/3}$, $\langle N_{sw} \rangle^{(2/3-\alpha_m)}$, $\langle v_{sw} \rangle^{(7/3-2\alpha_m)}$, $\langle B_{sw} \rangle^{2\alpha_m}$, and $\langle \sin^4(\theta/2) \rangle$. We employ annual means rather than, for example, running means over 12 or 13 rotation periods [*Gazis*, 1996]. The latter would give smoother variations and would avoid a noise variation caused by the means being biased by the inclusion of half solar rotations. On the other hand, we wish to compare with the annual means of *aa* in which seasonal and annual effects have been averaged out. We therefore use annual means, which also have the advantage that each data point is entirely independent of the next. In the case of the IMF clock angle term, there could be two contributions to a long-term change in θ in that the IMF orientation in GSE coordinates could have changed and/or the orientation of the GSM frame (with respect to the GSE frame) has changed because of the drift of the Earth's dipole axis. To evaluate the latter possibility we also evaluate $\langle \sin^4(\theta_{95}/2) \rangle$, where θ_{95} are the values of θ computed for all hourly data using the IGRF model coefficients for 1995.

The term dependent on Earth's magnetic moment $\langle M_E \rangle^{2/3}$ (Figure10a) shows a gradual decrease to lower values, as does the coupling term dependent on the IMF orientation (in GSM coordinates), $\langle \sin^4(\theta/2) \rangle$ (Figure 10f). As there is no significant difference between $\langle \sin^4(\theta/2) \rangle$ and $\langle \sin^4(\theta_{95}/2) \rangle$, we can discount the motion of the Earth's magnetic axis as a factor and thus the decrease in $\langle \sin^4(\theta/2) \rangle$ is due to changes in the orientation of the IMF in the GSE frame. These two decreases are more than compensated for by rises in the other terms of equation (5). The solar wind density term $\langle N_{sw} \rangle^{(2/3-\alpha_m)}$ (Figure 10b) shows a gradual but slight rise in cycles 21 and 22 but is especially low in cycle 20, making the overall rise larger. *Hapgood et al.* [1991] noted that the minimum in dynamic pressure P_{sw} seen around the peak of cycle 20 (1969) was due to a marked minimum N_{sw} with very little variation in v_{sw} whereas the minimum P_{sw} near the peak of cycle 21 (1980) was due to a marked minimum v_{sw} with very little variation in N_{sw}. Comparison of Figures 10b and 10c shows that cycle 22 was more like cycle 21, with low v_{sw} at its peak (1990), but no minimum in N_{sw}. Very little solar cycle variation can be seen in N_{sw}, a result that initially appears surprising considering that coronal mass ejections are thought to carry a significant fraction (of order 2-20%, depending on the phase of the solar cycle) of the solar wind mass and their occurrence shows a strong solar cycle variation [*Webb and Howard*, 1994]. This is because CMEs expand as they traverse interplanetary space, and so N_{sw} within each CME falls and because the Earth remains immersed in the high N_{sw} streamer belt at sunspot minimum. Figure 10 also confirms that the mean v_{sw} is large in the declining phase of cycle 22, confirming the association with the increased occur-

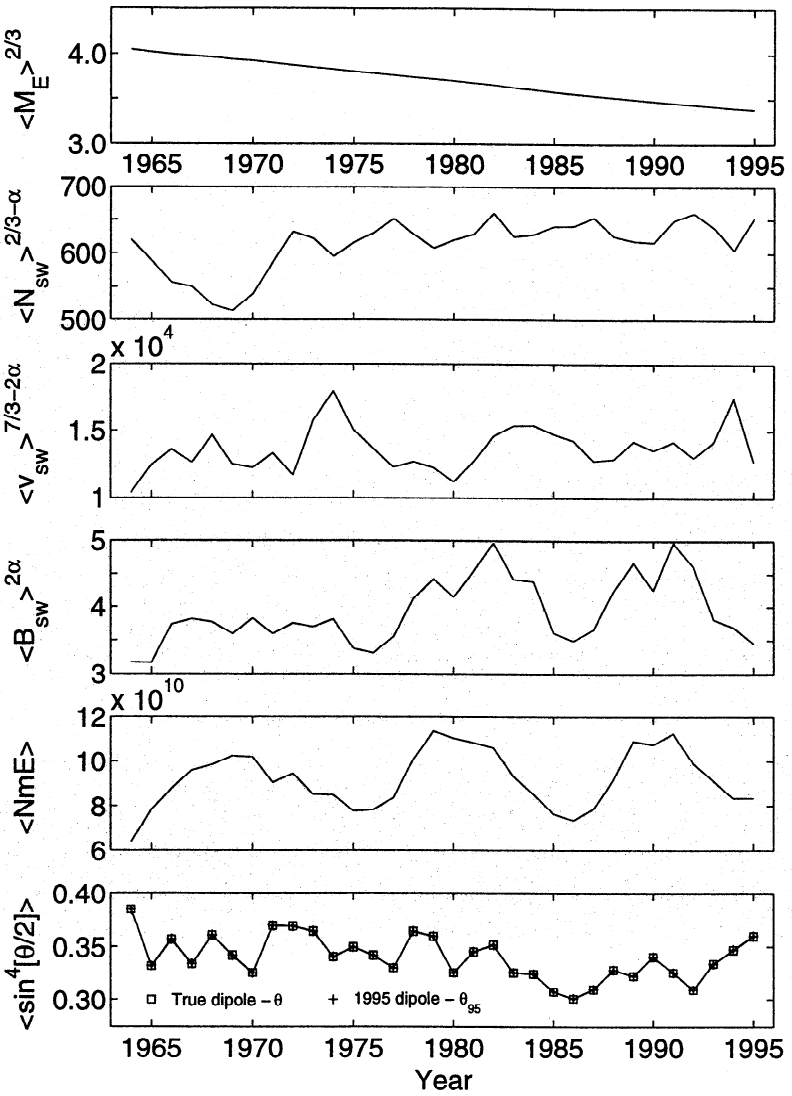

Figure 10. The variations of the annual means of the various terms of the bestfit coupling function P_m: (a) $\langle M_E \rangle^{2/3}$; (b) $\langle N_{sw} \rangle^{(2/3-\alpha m)}$; (c) $\langle v_{sw} \rangle^{(7/3-2\alpha m)}$; (d) $\langle B_{sw} \rangle^{2\alpha m}$; (f) $\langle \sin^4[\theta/2] \rangle$ (open squares and solid line) . Also shown in Figure 10f is $\langle \sin^4[\theta_{95}/2] \rangle$ (crosses). (e) The annual mean E layer peak density seen at Slough/Chilton, N_mE.

rence of recurrent storms in the declining phase of even-numbered solar cycles [*Hapgood*, 1993].

The term dependent on the solar wind speed $\langle v_{sw} \rangle^{(7/3-2\alpha m)}$ (Figure 10c) also shows as pronounced a drift to larger values over these three solar cycles. The term dependent on the IMF magnitude, $\langle B_{sw} \rangle^{2\alpha m}$ (Figure 10d) shows a drift to larger values, and a clear solar cycle variation. At the peak of cycle 20, relatively small values of B_{sw} are observed, as noted by *Crooker and Gringauz* [1993] and *Hapgood et al.* [1991]. As for the behavior of v_{sw} and N_{sw}, cycle 22 is much more similar to cycle 21 in this respect.

In order to quantify the drifts in the various terms in P_m seen in Figure 10, we assume that all the longer-term changes are approximately linear over the three solar cycles for which we have IMF and solar wind data. Because the period covers three full cycles, we can carry out a linear regression fit to the data sequence for each term, X, giving a mean gradient with time, $s_X \pm e_s$ (use of part of a cycle would bias the value of s_X). Thus, over the period of the study (Δt long), there will have been a total drift of $(s_X \pm e_s)\Delta t$. Table 2 gives the fitted gradients and also expresses the change as a percentage of the mean value for the period, $c_X = \{100\Delta t(s_x \pm e_s)/\langle X \rangle\}$. We define s_X (and thus c_X) as being positive if X drifts to larger values.

The errors in the fitted slopes and percentage changes are mainly caused by solar cycle variations. Therefore the error in the drift of $M_E^{2/3}$ is much less than that in other terms. As noted previously, the calibration of the solar wind density measurements prior to 1974 is more uncertain and Figure 10 shows that these data for cycle 20 add considerably to the overall gradient in N_{sw} . We also note from Figure 9 that the fit of P_m to $\langle aa \rangle$ is much poorer before 1974. If we remove the first 11 values of the N_{sw} variation (i.e. cycle 20), the percentage change c_{Nsw} falls to +3.16% (were all three cycles the same, we would expect a fall by one third, i.e. to about 9%). However, the percentage change in $\langle aa \rangle$ also falls by more than a third, to $c_{\langle aa \rangle} = 16.47\%$.

Table 2 shows that the effect of the change in the Earth's magnetic moment would, on its own, have reduced the power input to the magnetosphere by 1.7%. In addition, the change

Table 2. Fitted Percentage Change Over the Period 1964-1996 for Various Parameters for Best Fit Alpha $\alpha = \alpha_m = 0.386$

Parameter X	Units of X	Mean $\langle X \rangle$	Slope s_X, units/yr^{-1}	Percent Change, c_X
$\langle aa \rangle$	NT	23.693	$+0.29 \pm 0.080$	39.0 ± 10.5
$M_E^{2/3}$	$(\mathrm{Tm}^3)^{2/3}$	3.971×10^{10}	$-(2.1827 \pm 0.010)\times10^{7}$	-1.704 ± 0.008
$N_{sw}^{(2/3-\alpha m)}$	$(\mathrm{m}^{-3})^{(2/3-\alpha m)}$	6.145×10^{2}	2.7 ± 0.57	13.7 ± 2.9
$v_{sw}^{(7/3-2\alpha m)}$	$(\mathrm{km\ s}^{-1})^{(7/3-2\alpha m)}$	1.367×10^{4}	50.42 ± 30.82	11.4 ± 7.0
$B_{sw}^{2\alpha m}$	$(\mathrm{nT})^{2\alpha m}$	3.929	$(2.43 \pm 0.85)\times10^{-2}$	19.1 ± 6.7
$\sin^4(\theta/2)$	-	0.340	$-(1.02 \pm 0.35)\times10^{-3}$	-9.3 ± 3.2
$\sin^4(\theta_{95}/2)$	-	0.340	$-(1.02 \pm 0.35)\times10^{-3}$	-9.3 ± 3.2
R	-	72.500	0.786 ± 0.956	33.6 ± 40.9
N_mE	(m^{-3})	9.217×10^{10}	$(2.463 \pm 2.466)\times10^{8}$	8.3 ± 8.3
$\lvert B_x \rvert$	(nT)	3.315	0.035 ± 0.009	32.8 ± 8.4
C	(counts hr^{-1})	3933	-3.48 ± 3.30	-3.71 ± 3.51

in the IMF orientation reduced the power input by a further 9.3%. However, these decreases are more than compensated for by effects of the rises in the terms due B_{sw} (19.1%), v_{sw} (11.4%), and N_{sw}, (13.7%).

The peak E layer density observed at Slough/Chilton, N_mE, also rose by 8.3% in this period. The regression fit to the sunspot numbers gave a drift in mean values over the period 1964-1996 from $R_1 = 59$ to $R_2 = 85$. Putting this into equation (2) would give a ratio of the corresponding mean N_mE values $\{N_mE_1/N_mE_2\} = 0.94$, equivalent to a percentage change of 7.5%. Thus the change in mean E layer densities is roughly what we would expect from the rise in sunspot numbers. We can use the variation of a_n with N_mE, as shown in Figure 5, to calibrate the effect that this had on the mean aa values:

$$|\partial\langle aa\rangle/\partial t|_{NmE} = \{\partial N_mE/\partial t\}\{\partial\langle aa\rangle/\partial N_mE\} \approx \{\partial N_mE/\partial t\}\, s_{an}. \quad (7)$$

Using the value for s_{an} of 6.560×10^{-11} nT m^3 derived earlier, we derive the rate of change of $\langle aa \rangle$ due to changes in E layer densities is 0.0161 nT yr^{-1} which corresponds to a percentage change of 2.17% over the three solar cycles (i.e., a multiplying factor of $f_{NmE} = 1.022$).

Therefore the factors causing the change in geomagnetic activity (in order of their contribution to the upward drift in aa) are B_{sw}, N_{sw}, v_{sw}, N_mE, M_E, and θ. From Table 2 we find that over the three solar cycles, changes in these parameters multiply the average aa by factors of $f_{Bsw} = 1.191$, $f_{Nsw} = 1.137$, $f_{Vsw} = 1.114$, $f_{NmE} = 1.022$, $f_{ME} = 0.983$, and $f_\theta = 0.907$. The product of these factors $\{f_{Bsw}f_{Nsw}f_{Vsw}f_{NmE}f_{ME}f_\theta\} = 1.374$ and thus together they explain virtually the entire 39% rise in aa observed over solar cycles 20-22.

5. Discussion

We are now in a position to analyse the cause of the change in geomagnetic activity over solar cycles 20, 21, and 22 and from there make strong inferences about the change observed since cycle 11. We will look at all of the potential changes discussed in the introduction.

5.1. Changes in Instruments and Processing

Cross-calibration of the data from the different sites sets tight limits on the drift that could have been introduced by such effects. For the last three cycles studied in detail here, the exceptionally high correlation with annual averages of the auroral electrojet index AE means these effects are not a factor. (AE is recorded with different instruments, at different sites, and the data are processed in a different way). Use of annual means of daily averages of aa eliminates diurnal and annual periodicities in the data.

5.2. Changes in the Ionosphere

The long data sequence of E region critical frequencies from Slough/Chilton show some long-term changes, consistent with the known dependence on sunspot numbers through the changes in the photoionising solar electromagnetic flux. Comparison with daily means on N_mE and the northern hemisphere a_n index shows there is only an effect at low magnetic activities. Using this to calibrate dependence $\langle aa \rangle$ on N_mE shows that it is responsible for a change in average aa values of only 2.2% in the period 1964-1996, compared to the observed 39% change in $\langle aa \rangle$. In addition, the N_mE values vary in phase with the sunspot number. Thus E layer density changes due to changes in the EUV and X-ray solar flux offer an explanation of neither the drift nor the phase shift in geomagnetic activity.

Although the above eliminates changes in one of the variables controlling the local ionospheric conductivity (namely the E region plasma density) it is not a direct measure of the conductivity itself. Changes in the neutral thermosphere cannot be directly ruled out. The drift in the average K values for the southern hemisphere station (quantified by the a_s index) is almost identical to that for the northern hemisphere (quantified by the a_n index) and therefore to that for the aa index. To explain this close similarity of a_s and a_n, thermospheric changes would need to be the same at the two antipodal locations and so global in scope. The small difference between a_s and a_n could arise from the effects of local magnetic field changes on the conductivity, but this does not offer an explanation of the main drift of both. The very high correlation that we are able to obtain between the predicted power input to the magnetosphere and the $\langle aa \rangle$ values shows that any long-term drifts in the ionospheric conductivity effects are indeed very small. Direct effects of the height of the conducting layer are also negligible.

5.3. Changes in the Magnetosphere

We have no direct evidence that can rule out the possibility that the drift in geomagnetic activity, at least partially, reflects a change in the magnetospheric response to constant energy

input. However, we note that we have obtained an unprecedentedly strong and significant correlation with an input power coupling function, using a coupling exponent that is not greatly different for that found in studies of higher time resolution data. This correlation can explain 93% of the observed variation. The remaining 7% will include random fluctuations (including measurement uncertainties) as well as the effects of periodic fluctuations and long-term drifts in the magnetospheric response, the mean ion mass of the solar wind and the ionospheric conductivities. We estimated in the previous section that in the unexplained 7% there is a 2.2% long-term drift introduced by the increase in ionospheric conductivities produced by photoionization. Therefore, although we cannot completely rule out long-term changes in the magnetospheric response, we certainly find no evidence for them here and can set a low upper limit on their contribution to the net drift in geomagnetic activity.

5.4. Changes in Energy Coupling to the Magnetosphere

We have found a slight decrease in the IMF clock-angle factor which controls the energy input to the magnetosphere. This drift is relatively small and is in the opposite sense to that required to explain the drift in geomagnetic activity. Although the coupling function at any one time can be greatly in error if the geomagnetic field orientation for the wrong epoch is used, we find that these errors are averaged out in the annual means. Thus the drift in the orientation of the Earth's dipole axis is not a factor and the change purely reflects an slight tendency for the IMF to increasingly lie in the ecliptic plane. The area that the magnetosphere presents to the solar wind flow has decreased. This is partly because of a drop in the Earth's magnetic moment, but mainly due to a gradual rise in the solar wind dynamic pressure which compresses the magnetosphere. Both these factors are included in the best fit coupling function, P_m.

5.5. Changes in the Interplanetary Medium at 1 AU

The effects of the decrease in the IMF-orientation transfer function and the Earth magnetic moment are more than compensated for by a steady rise in the solar wind speed, density, and the IMF strength seen at 1 AU. This drift is superimposed on solar cycle effects that are very similar in cycles 21 and 22, but strikingly different for cycle 20. The biggest factor in the rise in geomagnetic activity is the rise in the strength of the IMF at the Earth. Several authors have noted that geomagnetic activity, as quantified by the number of major storms, often shows two peaks in a solar cycle, one in the rising phase and one in the declining phase [*Gonzales et al.*, 1990]. *Schreiber* [1998] associates these with increases in average B_s and v_{sw}, respectively. Figure 10 shows that the rise in B_s is due to rises in the IMF strength B_{sw} with no clear effect of the IMF orientation (in the GSM frame), but that these rises are largely in phase with the solar cycle. The phase delay in the average activity arises largely from the increased mean v_{sw} associated with the high-speed flow streams (and recurrent storms) in the declining phase, particularly for cycles 20 and 22 [*Cliver et al.*, 1996].

5.6. Changes in the Sun

It is interesting to note that there is an upward drift in both the interplanetary magnetic field strength and the solar wind speed at the Earth. The simple theory of the IMF Parker spiral successfully predicts the average orientation on the IMF in the *X-Y* GSE plane and the radial and latitudinal variations of the IMF in the inner heliosphere [*Gazis*, 1996; *Burlaga et al.*, 1998]. According to this theory, the IMF magnitude is given by

$$B_{sw} = \{B_r^2 + B_\phi^2\}^{1/2} = B_0 (R_0/r)^2 \{1 + (\omega r \cos\theta / v_{sw})^2\}^{1/2}, \quad (8)$$

where B_r is the radial component of the IMF, B_ϕ is the azimuthal component, ω is the angular velocity of solar rotation, θ is the heliographic latitude, B_0 is the field at the coronal source sphere at a heliocentric distance of R_0 (where the solar field becomes purely radial), and r = 1 AU at the Earth. Equation (8) is based on radial solar wind flow which applies for the annual means. It predicts that an increase in solar wind speed v_{sw} would cause a decrease in the IMF B_{sw} if the coronal source field B_0 is constant. *Luhmann et al.* [1993] noted that v_{sw} and B_{sw} were not always perfectly anti-correlated, implying variations in B_0. Table 2 shows that in fact, both have increased on average and this leads us to suggest that the average coronal source field, B_0, has increased, as well as the mean velocity which the solar wind is ejected. *Bowe et al.* [1990] showed that average v_{sw} and B_{sw} were indeed anticorrelated, as predicted by the simple Parker spiral theory, but only for the range of IMF values between ~4 and 9 nT. At B_{sw} < 4nT and B_{sw} > 9nT, v_{sw} and B_{sw} tended to increase together. In addition, they showed that N_{sw} and B_{sw} increased together at B_{sw} > 4nT but were strongly anti-correlated at B_{sw} < 4nT. Therefore the range of B_{sw} for which N_{sw}, B_{sw}, and v_{sw} all increased together in an average sense was B_{sw} > 9 nT. This may offer a clue as to which elements of the solar wind have contributed most to the observed drifts in the averages (magnetic clouds, coronal mass ejections, high-speed flow streams, corotating interaction regions, quiet streamer-belt solar wind, etc.). Such a study is beyond the scope of the present paper.

Figure 11 demonstrates how well the Parker spiral predicted by equation (8) matches the annual means of the IMF seen near Earth. Figure 11a shows the mean IMF B_z (=B_θ) in GSE coordinates and the mean of the modulus of B_z (<|B_z|>). Although the former shows the solar cycle variation in out-of-ecliptic field associated with B_{sw}, the latter is always close to zero because the distribution is symmetric about zero [*Hapgood et al.*, 1991] making $B_z = B_\theta \approx 0$ for all years. Figure 11c shows the variations of the mean of the IMF garden-hose angle in the X-Y GSE frame. The solid line is the annual means of the angle with respect to the -X direction, <γ>, predicted from hourly averages of the solar wind flow speed using equation (8) (where $\gamma = \tan^{-1}\{|B_x|/B_y\} = \tan^{-1}\{|B_r|/B_\phi\} = \tan^{-1}\{v_{sw}/\omega r\}$). The dashed line is (<$\gamma$>+<$\delta$>), where δ is the hourly mean of the deviation of the observed IMF orientation in the X-Y plane from the predicted one. Figures 11a and 11c shows that the annual means of the IMF orientation are always close to that predicted by Parker spiral theory. Figure 11b shows the annual means of $|B_x| = |B_r|$. By Parker spiral theory, $|B_r| = |B_0|(R_0/r)^2$, and thus the variations reflect the source field B_0. A linear regression fit to Figure 11b (dashed line) yields a percentage change in B_0 of c_{B_0} = 33% (Table 2). Results from the Ulysses satellite have shown that the heliospheric field is approximately independent of solar latitude and longitude [*Balogh et al.*, 1995]. This spherical symmetry means that the percentage rise in B_0 reflects a similar rise in the total open flux of the sun [*Wang and Sheeley*, 1995]. The lack of a latitudinal variation of the heliospheric field also

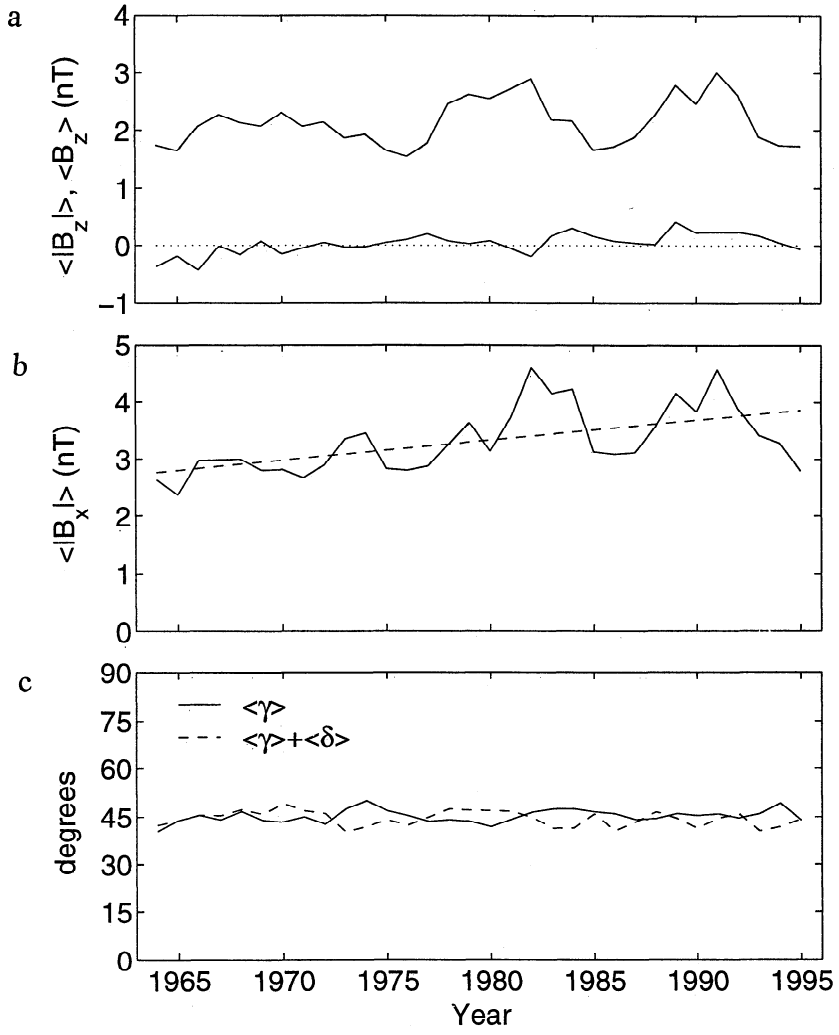

Figure 11. Annual means of the IMF seen at r = 1 AU in GSE coordinates: (a) $\langle B_z \rangle$ (which is always close to zero) and $\langle |B_z| \rangle$. (b) $|B_x| = |B_r|$. (c) The mean of the IMF garden-hose angle in the *X-Y* GSE frame: predicted from Parker spiral theory $\langle \gamma \rangle$ (solid line) and observed $\langle \gamma \rangle + \langle \delta \rangle$ (dashed line).

shows that there are no significant volume currents and only sheet currents are present. *Wang and Sheeley* [1995] employed this finding, along with an improved correction for limb effects, to map the observed photospheric fields to the coronal source sphere (at radius R_0). These mapped source field variations match closely the radial field seen at Earth between 1970 and 1994 (see their Figure 2b). Although the Wang and Sheeley did not comment on it, we note that their modeled coronal source field also shows the drift to larger values, which we here highlight in Figure 11b.

The flux of galactic cosmic rays is well known to be anticorrelated with the sunspot numbers because the Earth is more shielded from cosmic rays at sunspot maximum by the heliosphere. Figure 12 shows the normalized variation C^* of the cosmic ray flux detected at the Climax station in Colorado, *C*, for 1953-1996. Because of the anticorrelation, we plot $-C^*$ in Figure 12a as a solid line, R^* is given as a dashed line. There are a number of mechanisms that contribute to the cosmic ray shielding. The particles are scattered by irregularities in the heliospheric field, they are convected and decelerated by the solar wind, and they suffer gradient and curvature drifts because of the large-scale structure of the heliospheric field. The relative importance of the various effects is not yet clear (see review by *Moraal* [1993]), although we note *Cane et al.* [1999] find that long-term cosmic ray flux variations reflect changes in the coronal source magnetic flux. Figure 12 shows not only a solar cycle variation in the flux *C* but also a significant drift to lower values. This can be seen in the maximum C^* seen at sunspot minimum and, to an even greater extent, in the minimum C^* seen at sunspot maximum. A regression fit to the *C* values over the period 1964-1996 (as for the other parameters in Table 2) gives a percentage change of -3.7% of the mean value. This should be compared with the amplitude of the solar cycle variation which, for example, for cycle 21 is 19%. Thus the cosmic rays show a significant drift to lower values, consistent with the rise in heliospheric fields inferred here. Figure 12b shows the difference between the normalised variation $-C^*$ and R^*. As for aa^*, there are oscillations caused by a tendency for cosmic ray flux changes to lag behind the sunspot cycle. However, this lag is only seen in the odd-numbered cycles, whereas the lag in $\langle aa \rangle$ (largely caused by recurrent storms) is usually greater in even-

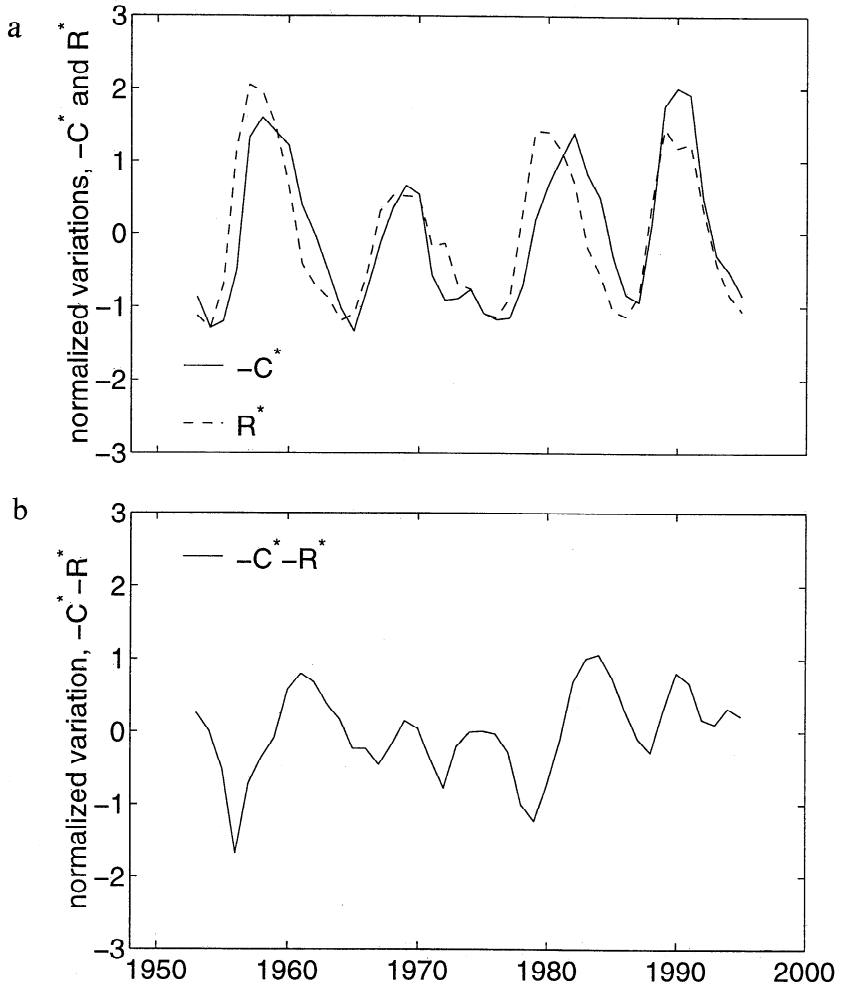

Figure 12. (a).The normalized Climax cosmic ray flux -*C** (see equation (1) of text) for the years 1953-1996 (solid line) and the normalized sunspot number, *R** (dashed line). (b). The difference (-*C** -*R**).

numbered cycles [*Cliver et al.*, 1996]. Figure 12b shows a gradual upward drift in the difference between these normalized variations, showing that the percentage fall in *C* exceeds the percentage rise in *R* in magnitude (as does the rise in <*aa*>).

6. Conclusions

From the similarity of the increases seen in the *aa* index and in the average sunspot numbers, one could infer that the drift in geomagnetic activity is caused by changes in the Sun itself. In this paper, we have studied the rise in *aa* over cycles 20, 21, and 22 using near-Earth interplanetary measurements. We find that the largest factor contributing to this rise, causing the roughly half of the rise in geomagnetic activity over these three solar cycles, is a rise in the IMF field strength; the other half arising from increases in the solar wind speed and density. However, the IMF orientation has grown somewhat less favorable for causing geomagnetic activity: this is because the mode value of the IMF clock angle in the GSM frame of reference has remained near 90° (i.e., the most common IMF orientation is in the ecliptic plane for all years), but the distribution width is lower (i.e., out of ecliptic field of either sense has grown slightly less common).

Other potential factors which could have contributed to the drift have been analyzed in detail and small upper limits placed on their net effect. We can conclude that the upward drift in geomagnetic activity is caused by changes in near-Earth interplanetary space.

Because Parker spiral theory applies to the annual averages studied, we can associate the rise in the IMF magnitude with a significant increase in the solar coronal source magnetic flux. This is consistent with a rise in the coronal source field, modeled from photospheric observations, and an observed decay in cosmic ray fluxes.

Because the percentage drift in <*aa*> values mirrors the drift in mean sunspot numbers, not only for the period 1964-1996 studied here but also for the full *aa* data sequence (Figure 1), the century-long drift in geomagnetic activity is most likely to reflect the same sort of changes in the Sun that we have found for the last three solar cycles. In a subsequent publication, *Lockwood et al.* [1999] exploit the conclusions reported here to extrapolate back to earlier solar cycles using the *aa* data and so investigate the variation of the solar coronal source flux since 1868.

Acknowledgments. The authors thank M. A. Hapgood of RAL for provision of the co-ordinate transformation software. The data used are stored and made available via World Data Centre, C1 for STP at

RAL, which is funded by the UK Particle Physics and Astronomy Research Council and, until April 1, 1999, by the National Radiowave Propagation Programme of the UK Radiocommunications Agency.

Michel Blanc thanks Nancy Crooker, Edward Cliver, and another referee for their assistance in evaluating this paper.

References

Akasofu, S.I., Energy coupling between the solar wind and the magnetosphere, *Space Sci. Rev., 28,* 121, 1981.

Allen, C.W., Critical frequencies, sunspots and the Sun's ultraviolet radiation, *J. Geophys. Res., 53,* 433-448, 1948.

Arnoldy, R. L., Signature in the interplanetary medium for substorms, *J. Geophys. Res., 76,* 5189-5201, 1971.

Baker, D. Statistical analyses in the study of solar wind-magnetosphere coupling, in *Solar Wind-Magnetosphere Coupling,* edited by Y. Kamide and J.A. Slavin, pp. 17-38, Terra Sci., Tokyo, 1986.

Balogh, A., E.J. Smith, B.T. Tsurutani, D.J. Southwood, R.J. Forsyth, and T.S. Horbury, The heliospheric field over the south polar region of the Sun, *Science, 268,* 1007-1010, 1995.

Bame, S.J., J.R. Asbridge, W.C. Feldman, and J.T. Gosling, Solar cycle evolution of high speed solar wind streams, *Astrophys. J.,* 207, 977, 1976.

Bargatze, L.F., R.L. McPherron, and D.N. Baker, Solar wind - magnetosphere energy input functions, in *Solar Wind-Magnetosphere Coupling,* edited by Y. Kamide and J.A. Slavin, pp. 101-109, Terra Sci., Tokyo, 1986 .

Baumjohann, W., Merits and limitations of the use of geomagnetic indices in solar wind- magnetosphere coupling studies, in *Solar Wind-Magnetosphere Coupling,* edited by Y. Kamide and J.A. Slavin, pp. 3-15, Terra Sci., Tokyo, 1986.

Bravo, S., and G.A. Stewart, The inclination of the heliomagnetic equator and the presence of an inclined relic field in the Sun, *Astrophys. J., 446,* 431, 1994.

Bremmer, J., Trends in the ionospheric *E* and *F* regions over Europe, *Ann. Geophys., 16,* 986-996, 1998.

Bowe, G. A., M. A. Hapgood, M. Lockwood, and D. M. Willis, Short-term variability of solar wind number density, speed and dynamic pressure as a function of the interplanetary magnetic field components: A survey over two solar cycles, *Geophys. Res. Lett., 17,* 1825-1828, 1990.

Burlaga, L.F., N.F. Ness, Y.-M. Wang, and N.R. Sheeley Jr., Heliospheric magnetic field strength out to 66 AU: Voyager 1, 1978-1996, *J. Geophys. Res., 103,* 23727-23732, 1998.

Cane H.V., G. Wibberenz, I.G. Richardson, and T.T. von Rosenvinge, Cosmic ray modulation and the solar magnetic field, *Geophys. Res. Lett., 26,* 565-568, 1999.

Cliver, E.W., V. Boriakoff, and K.H. Bounar, The 22-year cycle of geomagnetic activity, *J. Geophys. Res., 101,* 27091-27109, 1996.

Cliver, E.W., V. Boriakoff, and K.H. Bounar, Geomagnetic activity and the solar wind during the Maunder minimum, *Geophys. Res. Lett., 25,* 897-900, 1998.

Clilverd, M.A., T.D.G. Clark, E. Clarke, and H. Rishbeth, Increased magnetic storm activity from 1868 to 1995, *J. Atmos. Sol. Terr. Phys., 60,* 1047-1056, 1998.

Couzens, D. A., and J. H. King, *Interplanetary Medium Data Book - Supplement 3,* Nat. Space Sci. Data Cent., Goddard Space Flight Cent., Greenbelt, M., 1986.

Crooker, N.U., and K.I. Gringauz., On the low correlation between long-term averages of the solar wind speed and geomagnetic activity after 1976, *J. Geophys. Res., 98,* 59-62, 1993.

Crooker, N.U., J. Feynman, and J.A. Gosling, On the high correlation between long-term averages of solar wind speed and geomagnetic activity, *J. Geophys. Res., 82,* 1933-1937, 1977.

Davis, T.N., and M. Sigiura, Auroral electrojet index, *AE* and its universal time variations, *J. Geophys. Res., 71,* 785-801, 1966.

Ellis, W., The relation between magnetic disturbance and sunspot frequency, *Mon. Not. R. Astron. Soc. London., 60,* 142-157, 1900. (*Mon. Not. R. Astron. Soc. London,* 61, 538, 1900.)

Feynman, J., Solar cycle and long-term changes in the solar wind, *Rev. Geophys. 21,* 338-348, 1983.

Feynman, J., and N.U. Crooker, The solar wind at the turn of the century, *Nature, 275,* 626-627, 1978.

Friis-Christensen, E., and H. Svensmark, What do we really know about the sun-climate connection?, *Adv. Space Res., 20* (4/5), 913-920, 1997.

Fraser-Smith, A.C., Spectrum of the geomagnetic activity index *Ap, J. Geophys. Res., 77,* 4209-4220, 1972.

Gazis, P.R., Solar cycle variation of the heliosphere, *Rev. Geophys., 34,* 379-402, 1996.

Gonzales, W.D., I.C. Gonzales, and B.T. Tsurutani, Dual-peak solar cycle distribution of intense geomagnetic storms, *Planet. Space Sci., 38,* 181, 1990.

Gosling, J.T., J.R. Ashbridge, S.J. Bame, and W.C. Feldman, Solar wind speed variations 1962-1974, *J. Geophys. Res., 81,* 5061-5071, 1976.

Gosling, J.T., J.R. Ashbridge, and S.J. Bame, An unusual aspect of solar wind speed variations during solar cycle 20, *J. Geophys. Res., 82,* 3311-3314, 1977.

Gringauz, K.I., Average characteristics of the solar wind and its variation during the solar cycle, in *Solar Wind 4, Rep.* MPAE-W-100-81-31, edited by H. Rosenbauer, Max Planck Inst. fuer Aeron., Lindau, Germany, 1981.

Hapgood, M.A., A double solar-cycle variation in the 27-day recurrence of geomagnetic activity, *Ann Geophys., 11,* 248, 1993.

Hapgood, M.A., G. Bowe, M. Lockwood, D.M. Willis, and Y. Tulunay, Variability of the interplanetary magnetic field at 1 AU over 24 years: 1963-1986, *Planet. Space Sci., 39,* 411-423, 1991.

Hirshberg, J., and D.S. Colburn, Interplanetary field and geomagnetic variations – A unified view, *Planet. Space Sci., 17,* 1183-1206, 1969.

Hoeksema, J.T., Large-scale structure of the heliospheric magnetic field: 1976-1991, *in Solar Wind 7,* edited by E. Marsch and R. Schwenn, pp. 191-196, Pergamon, Tarrytown, New York, 1992.

Jarvis, M., B. Jenkins, and G.A. Rodgers, Southern hemisphere observations of a long-term decrease in *F*-region altitude and thermospheric wind providing possible evidence for thermospheric cooling, *J. Geophys. Res., 103,* 20774-20788, 1998.

Kan, J.R., and S.-I. Akasofu, Dynamo process governing solar wind magnetosphere coupling, *Planet. Space Sci., 30,* 367-370, 1982.

Lockwood, M., R. Stamper, and M.N. Wild, A doubling of the Suns' coronal magnetic field during this century, *Nature, 399,* 6735, 437-439, 1999.

Luhmann, J.G., T.-L. Zang, S.M. Petrinec, C.T. Russell, P. Gazis and A. Barnes, Solar cycle 21 effects on the interplanetary magnetic field and related parameters at 0.7 and 1.0 AU, *J. Geophys. Res., 98,* 5559-5572, 1993.

Mayaud, P.N., Une mésure planetaire d'activity magnetique, basée sur deux observatories antipodaux, *Ann. Geophys., 27,* 67-70, 1971.

Mayaud, P.N., The *aa* indices: A 100-year series characterising the magnetic activity, *J. Geophys. Res., 72,* 6870-6874, 1972.

Merrill, R.T., M.W. McElhinny, and P.L. McFadden, *The Magnetic Field of the Earth: Paleomagnetism, the Core, and the Deep Mantle,* p. 34, Academic, San Diego, Calif., 1996.

Moraal, H., Cosmic ray modulation studies in the outer heliosphere, *Nucl. Phys. B Proc. Suppl., 33A,B,* 161-178, 1993.

Mursula, K., and B. Zieger, The 13.5-day periodicity in the Sun, solar wind and geomagnetic activity: The last three solar cycles, *J. Geophys. Res., 101,* 27077-27090, 1996.

Muryama, Y., Coupling function between solar wind parameters and geomagnetic indices, *Rev. Geophys., 20,* 623-629, 1982.

Muryama, Y., and K. Hakamada, Effects of solar wind parameters on the development of magnetospheric substorms, *Planet. Space Sci., 23,* 75-91, 1975.

Neugebauer, M., Observations of solar wind helium, *Fund. Cosmic Phys., 7,* 131, 1981.

Nevanlinna, H., and E. Kataja, An extension to the geomagnetic activity index series *aa* for two solar cycles (1844-1868), *Geophys. Res. Lett., 20,* 2703-2706, 1993.

Perreault, P., and S.-I. Akasofu, A study of geomagnetic storms, *Geophys. J. R. Astron. Soc., 54,* 547-573, 1978.

Rishbeth, H., A greenhouse effect in the ionosphere?, *Planet Space Sci., 38,* 945-948, 1990.

Russell, C.T., On the possibility of deducing interplanetary and solar parameters from geomagnetic records, *Sol. Phys., 42*(1), 259-269, 1975.

Russell, C.T., and R.L. McPherron, Seasonal variation of geomagnetic activity, *J. Geophys. Res., 78,* 92-108, 1973.

Rosenberg, R.L., and P.J. Coleman, Heliographic latitude dependence

of the dominant polarity of the interplanetary magnetic field, *J. Geophys. Res., 74*, 5611, 1969.

Sabine, E., On what the colonial magnetic observatories have accomplished, *Proc. R. Soc. London, 19*, 1857.

Schield, M.A., Pressure balance between the solar wind and magnetosphere, *J. Geophys. Res., 74,* 1275, 1969.

Schatten, K. H., and J. W. Wilcox, Response of geomagnetic activity index *Kp* to interplanetary magnetic field, *J. Geophys. Res., 72,* 5185-5191, 1967.

Schreiber, H., On the periodic variations of geomagnetic activity indices *Ap* and *ap*, *Annales Geophys., 16*, 510-517, 1998.

Scurry L., and C.T. Russell, Proxy studies of energy transfer to the magnetosphere, *J. Geophys. Res., 96,* 9541-9548, 1991.

Sheeley, N.R., Jr., J.W. Harvey, and W.C. Feldman, Coronal holes, solar wind streams and recurrent geomagnetic disturbances, 1973-1976, *Sol. Phys., 49*(2), 271-278, 1976.

Slavin, J.A., G. Jungman, and E.J. Smith, The interplanetary magnetic field during solar cycle 21: ISEE-3/ICE observations, *Geophys. Res. Lett., 13,* 513, 1986.

Snyder, C.W., M. Neugebauer, and U.R. Rao, The solar wind velocity and its correlation with cosmic ray variations and with solar and geomagnetic activity, *J. Geophys. Res., 68*, 6360-6370, 1963.

Vasyluinas, V.M., J.R. Kan, G.L. Siscoe, and S.-I. Akasofu, Scaling relations governing magnetospheric energy transfer, *Planet Space Sci., 30*, 359-365, 1982.

Wang, Y.-M., and N.R. Sheeley Jr., Solar implications of Ulysses interplanetary field measurements, *Astrophys. J., 447*, L143-L146, 1995.

Wang, Y.-M., S.H. Hawley, and N.R. Sheeley Jr.,. The magnetic nature of coronal holes, *Science, 271*, 464-469, 1996.

Webb, D.F., and R.A. Howard, The solar cycle variation of coronal mass ejections and solar wind mass flux, *J. Geophys. Res., 99*, 4201, 1994.

T. D. G. Clark, British Geological Survey, Murchison House, West Mains Road, Edinburgh EH9 3LA, Scotland, UK. (T.Clark@bgs.ac.uk)

M. Lockwood, R. Stamper, and M. N. Wild, World Data Centre C-1 for Solar-Terrestrial Physics, Rutherford Appleton Laboratory, Chilton, Didcot, Oxfordshire OX11 0QX, UK. (M.Lockwood@rl.ac.uk; R.Stamper@rl.ac.uk; M.N.Wild@rl.ac.uk)

(Received December 1, 1998; revised June 22, 1999;
accepted June 28, 1999.)